

**Supplementary materials for**  
**Revisiting stepwise ocean oxygenation with authigenic Ba enrichments in marine**  
**mudrocks**

Guang-Yi Wei<sup>1\*</sup>, Hong-Fei Ling<sup>1\*</sup>, Graham A. Shields<sup>2</sup>, Simon V. Hohl<sup>3</sup>, Tao Yang<sup>1</sup>, Yi-Bo

Lin<sup>1</sup>, Feifei Zhang<sup>1</sup>

<sup>1</sup>*State Key Laboratory for Mineral Deposits Research, School of Earth Sciences and Engineering, Nanjing University, Nanjing 210023, China*

<sup>2</sup>*Department of Earth Sciences, University College London, Gower Street, London WC1E 6BT, U.K.*

<sup>3</sup>*State Key Laboratory of Marine Geology, School of Ocean and Earth Sciences, Tongji University, Shanghai 200092, China*

\*Email: G.-Y. Wei ([guangyiwei@nju.edu.cn](mailto:guangyiwei@nju.edu.cn)); H.-F. Ling ([hfling@nju.edu.cn](mailto:hfling@nju.edu.cn))

**DR1. Distinctions of different types of barite in marine sediments**

Scanning electron microscope (SEM) images of barite crystals separated from the different depositional environments exhibit varying morphologies and sizes (shown in Fig. DR1 from Paytan et al., 2002). Marine barite crystals deposited from water column are characterized by ellipsoidal in shape and small size (< 5–8  $\mu\text{m}$ ). Hydrothermal barite crystals are generally precipitated as cross-cutting tabular crystals and form rosettes with nobaly large crystal size (20–70  $\mu\text{m}$ ). Diagenetic barite crystals are larger (20–700  $\mu\text{m}$ ), flat, tabular-shaped and presented as barite beds in the sediments.

We check the SEM images of the early Cambrian black shales in South China with significant Ba enrichments (Figs. DR2,3). The particulate Ba in the early Cambrian black shales is presented as aggregates of barite with relative small crystal size and elliptical to sub-

spherical structures. Despite the potential diagenetic process during the black shale burial, morphological observations suggest a marine authigenic origin for the barites in the early Cambrian black shales. We also select those black shale and mudstone samples that are not altered by hydrothermal fluids based on the descriptions in published literature.

## **DR2. Material and methods**

New Ba concentration data were obtained from two early Cambrian organic-rich mudrock successions. Cherty shales, black shales and mudstones were collected from the Daotuo Drill core and the Yanjia section that were the same batches of samples in Wei et al. (2017) and (2020). These two sections are interpreted to have been deposited from the terminal Ediacaran to the lower Cambrian in a mid-depth margin–slope (Daotuo) to a deeper basin environment (Yanjia) on a continental margin. In order to avoid the contamination of Ba from authigenic carbonate, only bulk samples that have relatively low Ca concentrations (< 3%) were selected and ground into 200 mesh powders and then oven-dried at 60 °C for Ba concentration analysis. Approximately 50 mg of sample powder was weighed, then fully digested using distilled HF + HNO<sub>3</sub> + HCl acids. The solutions were dried and re-dissolved in 6 N HCl in preparation for element and isotope analyses. The Ba concentrations were measured on a Thermo Finnigan Element XR ICP-MS at the State Key Laboratory for Mineral Deposits Research, Nanjing University and the Yale Metal Geochemistry Center (YMGC), Yale University. The IAPSO seawater and USGS BHVO-2 standards were used to monitor the long-term reproducibility of the measurements (better than 5% in this study). The Ba<sub>excess</sub> data, along with published geochemical data in the Daotuo drillcore and Yanjia section are presented in Fig. DR4.

### **DR3. Compilations of Ba concentrations in shales and mudstones**

New analyzed and integrated data were presented in supplementary table with brief introduction and reference list in it.

### **DR4. Calculation of barite saturation index**

The saturation index of barites in the ocean was calculated in terms of the activity product of free Ba and SO<sub>4</sub> ions in the aqueous solution,

$$K_d = a_{Ba} \cdot a_{SO_4}$$

$$a_i = \Gamma_i(T, P) \cdot m_i = \gamma_i f_i \cdot m_i$$

where  $K_d$  is thermodynamic solubility product,  $a_i$  is the activity product of free ions,  $m_i$  is the product of the total molality,  $\gamma_i$  and  $\Gamma_i$  are the simple and apparent activity coefficients, respectively, which can be expressed as a function of temperature and pressure. Then the completed equation for barite saturation in the seawater can be defined as,

$$K_d(T, P) = (\gamma_{Ba} \cdot f_{Ba} \cdot m_{Ba}) \cdot (\gamma_{SO_4} \cdot f_{SO_4} \cdot m_{SO_4})$$

In this study, we use the values of  $K_d$ ,  $\gamma_{Ba}$ ,  $\gamma_{SO_4}$ ,  $f_{Ba}$ ,  $f_{SO_4}$  as  $1.1 \times 10^{-10}$ , 0.24, 0.17, 0.93, 0.39, respectively, assuming modern salinity and major ion concentrations, along with a temperature of 25 °C and a pressure of one atm for calculations (Church and Wolgemuth, 1972).

### **References**

Church, T. M., and Wolgemuth, K., 1972, Marine barite saturation: Earth and Planetary Science Letters, v. 15, no. 1, p. 35-44.

Paytan, A., Mearon, S., Cobb, K., and Kastner, M., 2002, Origin of marine barite deposits: Sr and S isotope characterization: *Geology*, v. 30, no. 8, p. 747-750.

Wei, G.-Y., Planavsky, N. J., Tarhan, L. G., He, T., Wang, D., Shields, G. A., Wei, W., and Ling, H.-F., 2020, Highly dynamic marine redox state through the Cambrian explosion highlighted by authigenic  $\delta^{238}\text{U}$  records: *Earth and Planetary Science Letters*, v. 544, p. 116361.

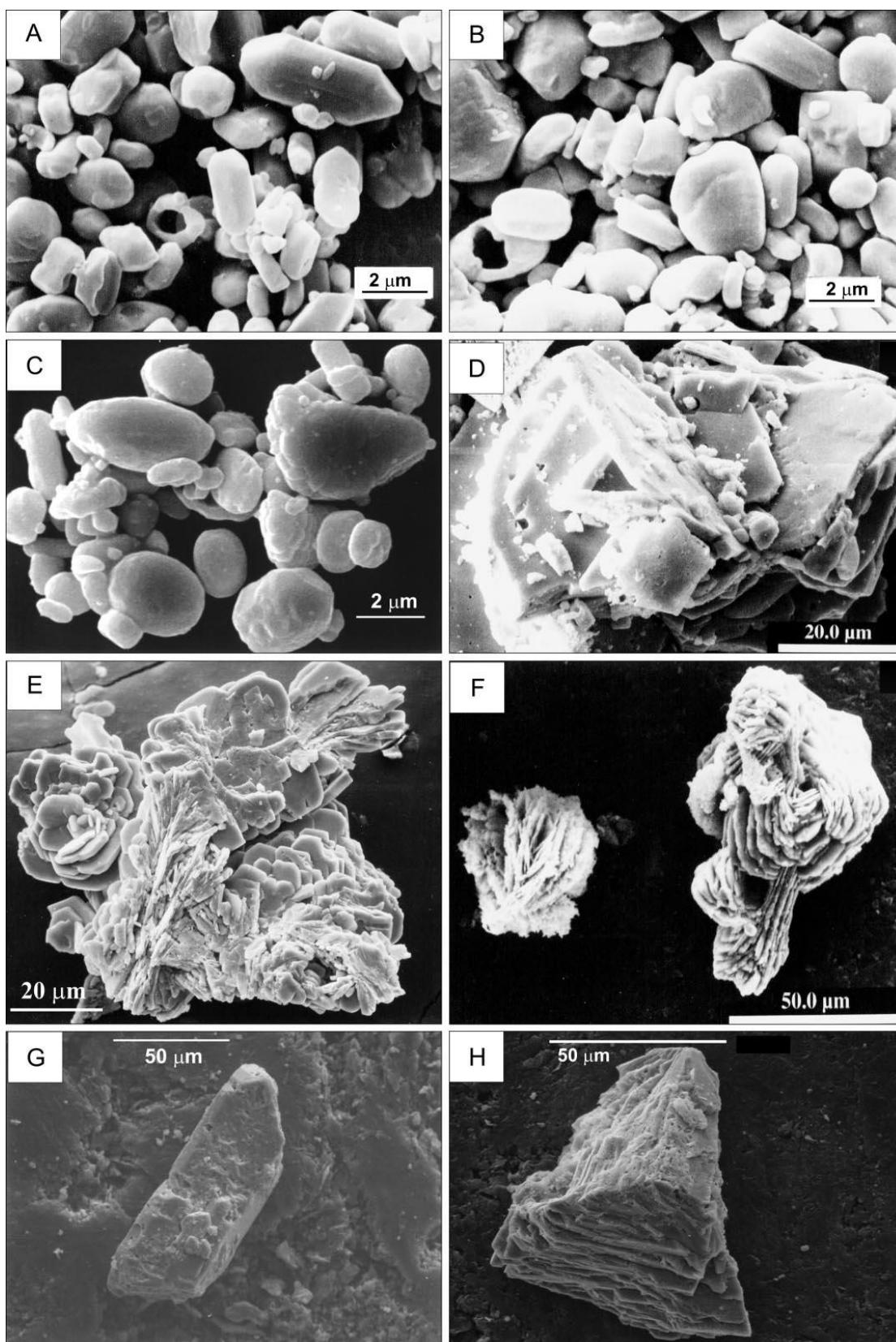


**Fig. DR1.** SEM (scanning electron microscopy) photographs of barite crystals from different modern oceanic settings (from Paytan et al., 2002). (A) (B) (C) are authigenic barites in marine sediments. (D) (E) (F) are hydrothermal barites near the hydrothermal chimneys. (G) (H) are diagenetic barites in marine sediments.

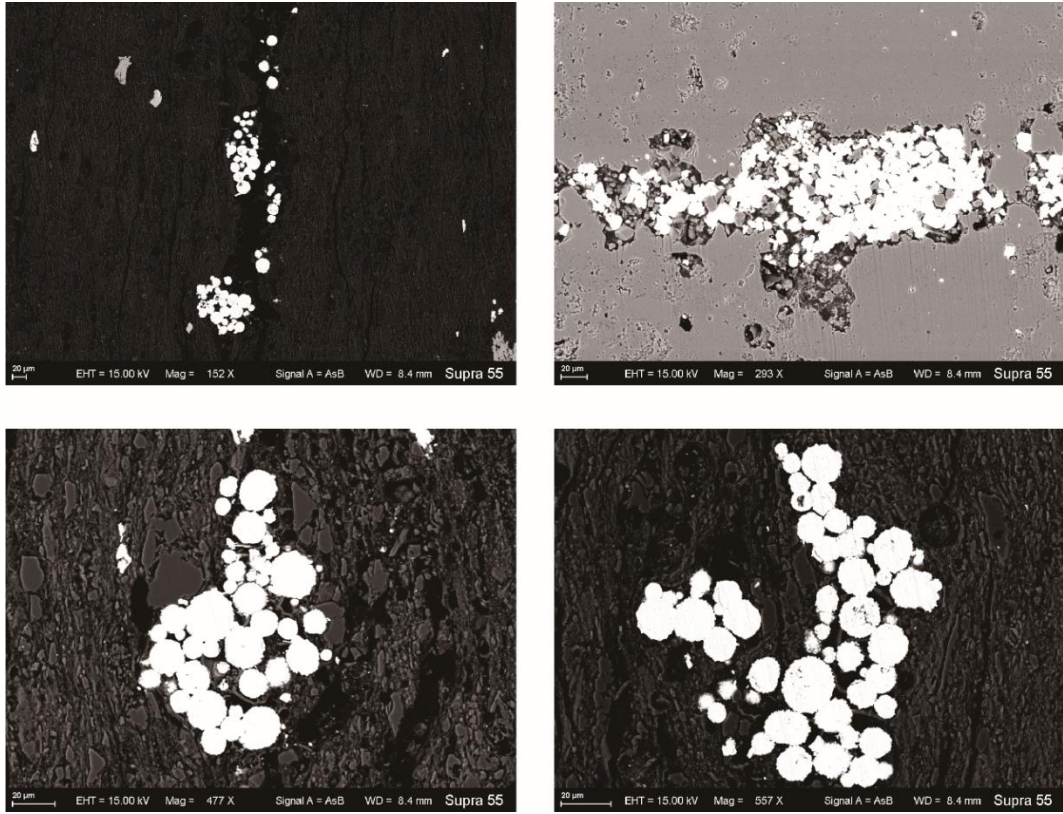


**Fig. DR2.** SEM (scanning electron microscopy) photographs of barite particles for black shales in the lower Cambrian in this study.

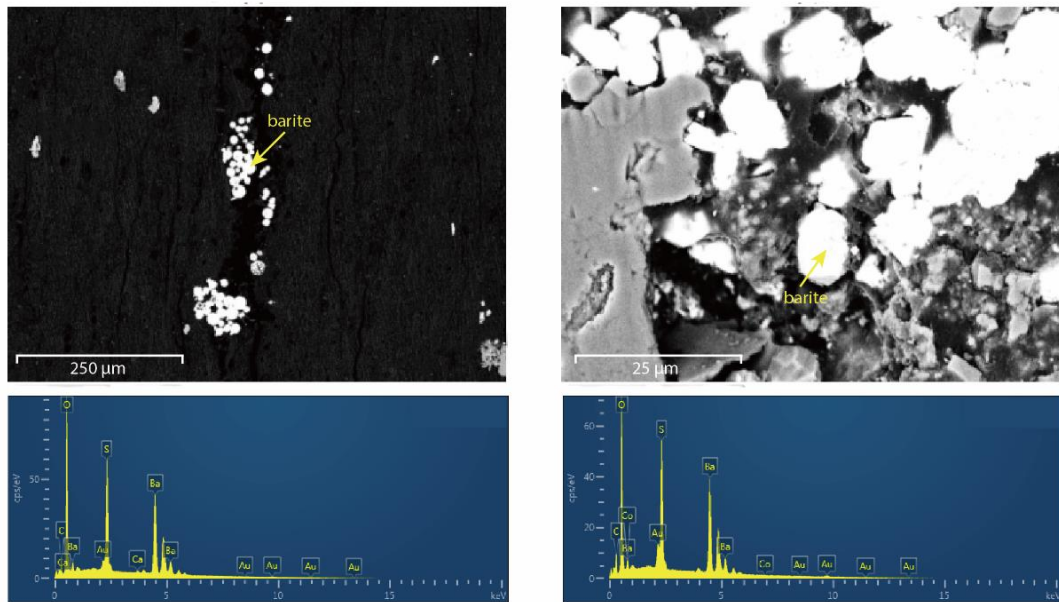


**Fig. DR3.** SEM photographs of barite particles for representative black shales in the lower Cambria. The barites in the samples are identified as peaks of O, S and Ba, using EDS (energy-dispersive spectrometry).

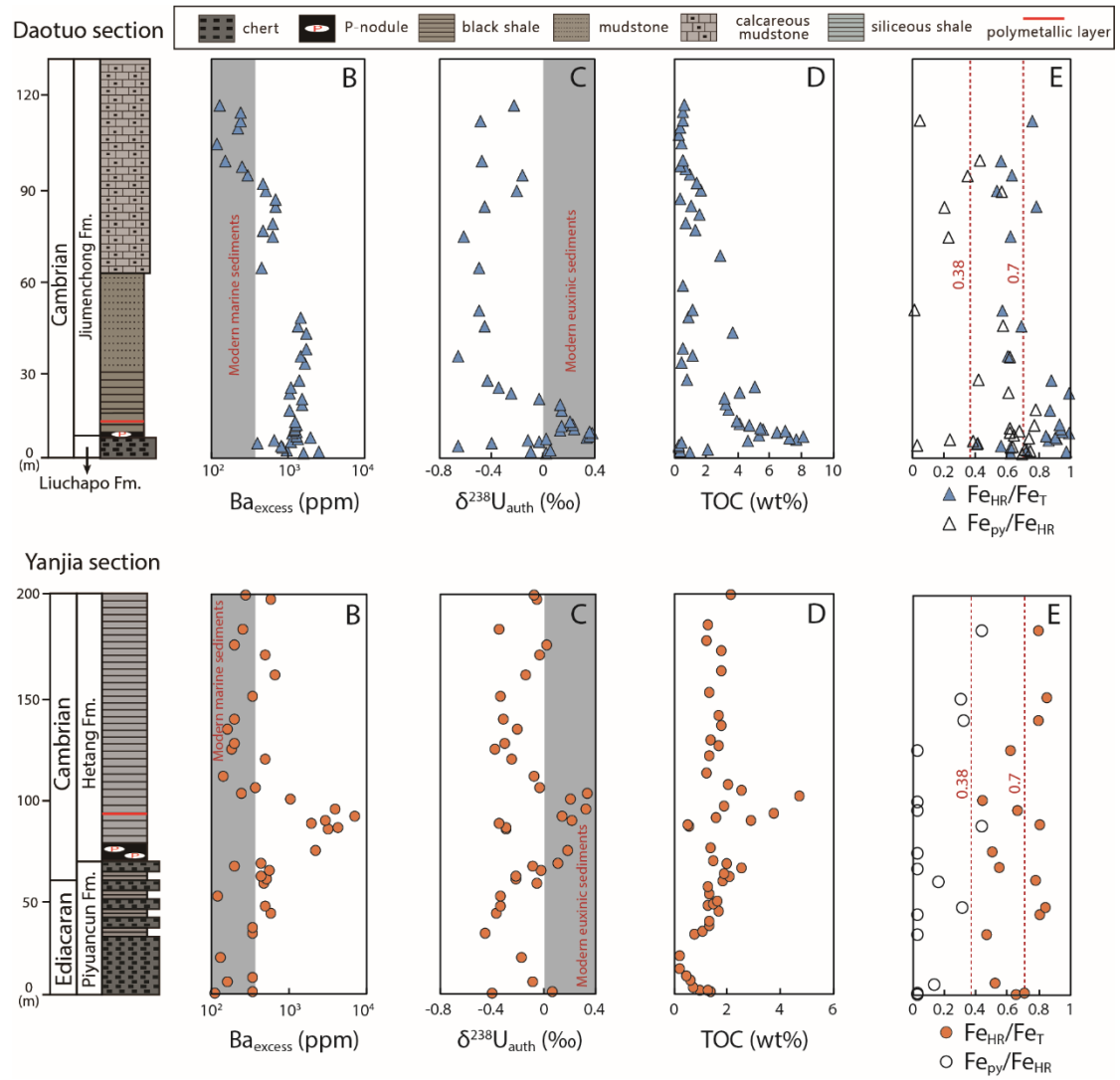


**Fig. DR4.** Geochemical profiles of the Daotuo drillcore and Yanjia section, including  $Ba_{excess}$  concentrations (this study), and U isotope, TOC, Fe speciation data (from Wei et al., 2020).

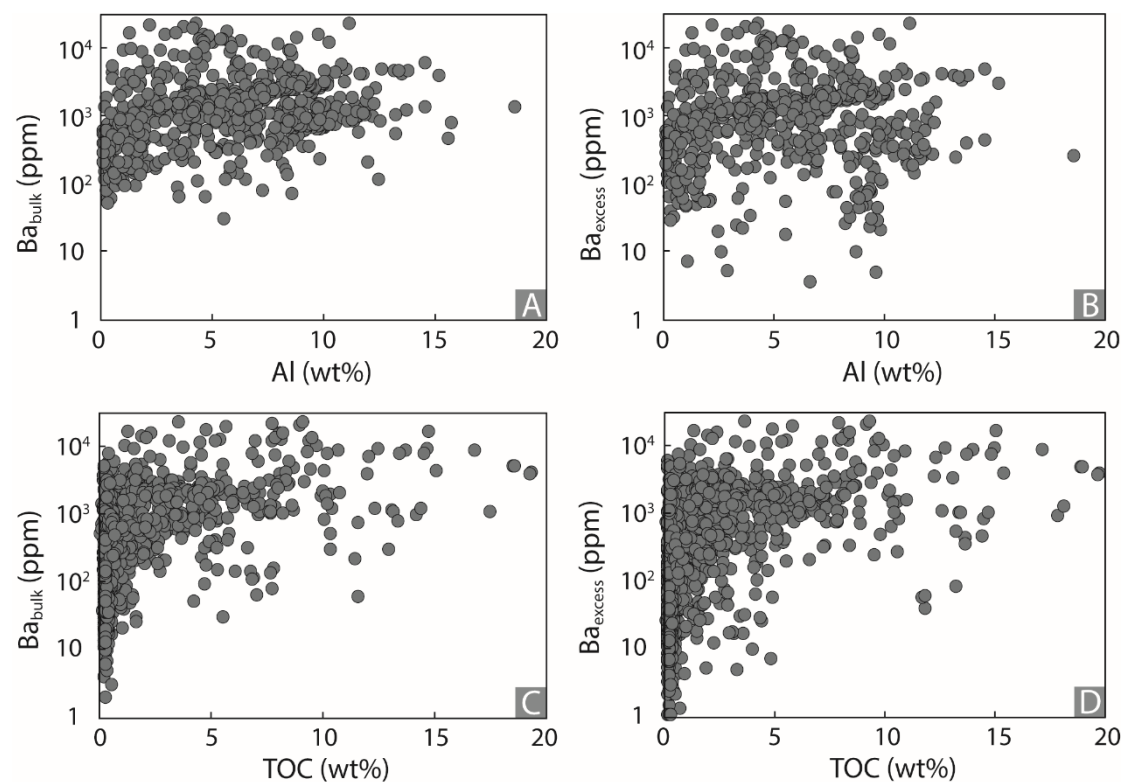


**Fig. DR5.** Cross-plots of (A)  $Ba_{bulk}$  vs. Al, (B)  $Ba_{excess}$  vs. Al, (C)  $Ba_{bulk}$  vs. TOC and (D)  $Ba_{excess}$  vs. TOC contents for the collected Neoproterozoic and Paleozoic samples.